This article has been accepted for publication in a future issue of this journal, but has not been fully edited. Content may change prior to final publication. Citation information: DOI 10.1109/JPHOT.2018.2824661, IEEE Photonics Journal

# Proposal of a phase-shift fiber Bragg grating as an optical Differentiator and an optical integrator simultaneously

**Xin Liu[1,2], Xuewen Shu[1,*], Hui Cao[3]**

[1]Wuhan National Laboratory for Optoelectronics & School of Optical and Electronic Information, Huazhong University of Science and Technology, Wuhan, 430074, China

[2]Aston Institute of Photonic Technologies, Aston University, Birmingham, B4 7ET

[3]School of Physics and Optoelectronic Engineering, Foshan University, Foshan 528000, China

*xshu@hust.edu.cn

**Abstract:** We show analytically and numerically that a practically realizable phase-shift fiber Bragg grating (PS-FBG) can function as a temporal first-order optical differentiator and a temporal first-order optical integrator at the same time. The PS-FBG working in reflection implements the differentiation and working in transmission implements the integration. We provide both the generalized conditions for a PS-FBG functioning as a first-order optical differentiator and a first-order optical integrator. The proposed PS-FBG can perform the time differential and integral of the complex envelope of an arbitrary input optical signal with high accuracy, respectively.

**Index Terms:** Fiber gratings, ultrafast devices, pulse shaping.

## 1. Introduction

All-optical signal processing offers a solution to overcome the speed limitation imposed by the electronics. Similar to the electronics, all optical circuit also need the fundamental elements, such as all-optical differentiator, all-optical integrator and so on. An optical differentiator is a device that performs real-time differentiation of the complex envelope and an optical integrator is a device that performs real-time integration of the complex envelope of an arbitrary input optical waveform. Recently, all-optical differentiators and integrators are both attracting great research interest due to their potential applications in pulse shaping, signal processing, and ultrafast optical signal coding [1-3].

Currently, a variety of schemes has been proposed to implement the all-optical differentiators and integrators. According to the platform of the device, those can be mainly classified into three categories: bulk optics based schemes (like interferometers) [4, 5], fiber platform based schemes (like fiber Bragg grating (FBG), long period grating (LPG)) [5-13], and on-chip platform based schemes (like silicon-on-isolator (SOI) microring resonator, InP–InGaAsP material system) [14-18]. Compared to other solutions, fiber-grating-based approaches offer some inherent advantages such as simplicity, low cost, low insertion loss, polarization independence, and inherent full compatibility with fiber optics systems.

However, the fiber platform based solutions that have been proposed previously all focus on separate functionality, which means that a device that function as a differentiator cannot function as an integrator at the same time.

In this paper, we propose the use of a phase-shift fiber Bragg grating (PS-FBG) for the first time to function as a first-order optical differentiator (OD) and a first-order optical integrator (OI) at the same time. The PS-FBG working in reflection implements the OD while the PS-FBG working in transmission implements the OI.

## 2. Principle

The transfer function of an ideal first-order OD and an ideal first-order OI are defined as [19], respectively

$$H_D(\omega) = j(\omega - \omega_0)$$
$$H_I(\omega) = \frac{1}{j(\omega - \omega_0)} \quad (1)$$

Where $j = \sqrt{-1}$ , $\omega$ is the angular optical frequency, $\omega_0$ is the angular central frequency and $\omega - \omega_0$ is the angular baseband frequency.

From Eq. (1), we can see that the amplitude response of an ideal first-order OD is linear dependence on the angular

This article has been accepted for publication in a future issue of this journal, but has not been fully edited. Content may change prior to final publication. Citation information: DOI 10.1109/JPHOT.2018.2824661, IEEE Photonics Journal

baseband frequency, while the amplitude response of an ideal first-order OI is inversely proportional to the angular baseband frequency. However, the phase responses of an ideal OD and an ideal OI both have a pi phase shift in the center angular frequency.

Fig. 1 shows the schematic of a PSFBG that consists of two concatenated FBGs (FBG1 and FBG2) with a phase shift $\phi$ between them. This PS-FBG can be described using the transfer matrix method [20].

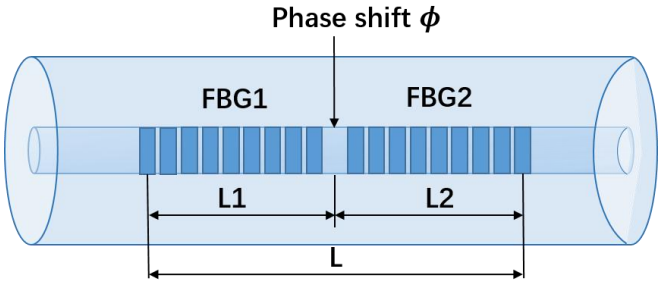


Fig. 1. Schematic of a phase-shift fiber Bragg grating.

The 2×2 transfer matrix $T$ of a PS-FBG can be given by

$$T = T_1 \cdot T_\phi \cdot T_2 \tag{2}$$

Where $T_1$, $T_2$, and $T_\phi$ are the 2×2 matrices of FBG1, FBG2 and the phase shift between the two gratings, respectively.

The elements of $T_m$ are given by

$$\begin{aligned} T_{m11} &= T_{m22}^{*} = \cosh(\gamma_m \Delta_m) - j(\sigma/\gamma_m)\sinh(\gamma_m \Delta_m) \\ T_{m12} &= T_{m21}^{*} = -j(\kappa_m/\gamma_m)\sinh(\gamma_m \Delta_m) \end{aligned} \tag{3}$$

Where ${\gamma_m}^2 = {\kappa_m}^2 - \sigma^2$. In the above expressions, $*$ denotes the complex conjugation, m = 1, 2 refers to the number of the grating, $\kappa_m$ is the coupling coefficient of the m-th grating, $\Delta_m$ is the corresponding grating length, $\sigma = 2\pi n_{eff}(\lambda^{-1} - \lambda_0^{-1})$ is the detuning from the Bragg wavelength $\lambda_0$ and $n_{eff}$ is the effective fiber mode index.

The elements of $T_\phi$ are given by

$$\begin{aligned} T_{\phi,11} &= T_{\phi,22}^{*} = \exp(-\mathrm{j}\phi/2) \\ T_{\phi,12} &= T_{\phi,21} = 0 \end{aligned} \tag{4}$$

The field reflectivity $r$ and transmittance $t$ of a PS-FBG structure can be obtained from its transfer matrix $T$ as

$$\begin{aligned} r &= \frac{T_{21}}{T_{22}} \\ t &= \frac{1}{T_{22}} \end{aligned} \tag{5}$$

The amplitude responses ($|r|$, $|t|$) and phase responses ($r_\theta$, $t_\theta$) of the reflectivity and transmittance are obtained from the field reflectivity $r$ and transmittance $t$ as

$$\begin{aligned} r &= |r| \cdot e^{ir_\theta} \\ t &= |t| \cdot e^{it_\theta} \end{aligned} \tag{6}$$

If we put the terms in Eq. (3) and Eq. (4) into Eq. (2), and then follow Eq. (5), we can get:

$$\begin{aligned} r &= \frac{j\kappa_1\kappa_2(|r_1| + |r_2|e^{j\phi}) + \sigma|r_1||r_2|(\kappa_1 - \kappa_2 e^{j\phi})}{\kappa_1\kappa_2(1 + |r_1||r_2|e^{j\phi}) - j\sigma(\kappa_1|r_1| + \kappa_2|r_2|) - \sigma^2|r_1||r_2|} \\ t &= \frac{\kappa_1\kappa_2\cosh(\kappa_1 L_1)\cosh(\kappa_2 L_2)e^{j\frac{\phi}{2}}}{\kappa_1\kappa_2(1 + |r_1||r_2|e^{j\phi}) - j\sigma(\kappa_1|r_1| + \kappa_2|r_2|) - \sigma^2|r_1||r_2|} \end{aligned} \tag{7}$$

Where $\kappa_i$, $L_i$ and $|r_i| = \tanh(\kappa_i L_i)$ ($i = 1, 2$) are the coupling coefficient, the grating length and the reflection peak of each uniform FBG section, respectively. The detuning from the center wavelength is $\sigma = 2\pi n_{eff}(\lambda^{-1} - \lambda_0^{-1}) = \frac{n_{eff}}{c}(\omega - \omega_0) \propto (\omega - \omega_0)$.

Here we show that for functioning as an ideal first-order OD the specification imposed in Ref. [7] (the two uniform FBGs in the structure must be identical ($L_1 = L_2 = L$ and $\kappa_1 = \kappa_2 = \kappa$), $\phi = \pi$) is not strictly necessary and we provide the generalized conditions for this operation ($\kappa_1 L_1 = \kappa_2 L_2$, $\phi = \pi + 2k\pi$).

From Eq. (7), in terms of the field reflectivity $r$, it can be inferred that in order to approach the spectral response that is required for the first-order OD, the following specification is necessary:

This article has been accepted for publication in a future issue of this journal, but has not been fully edited. Content may change prior to final publication. Citation information: DOI 10.1109/JPHOT.2018.2824661, IEEE Photonics Journal

$$|r_1| + |r_2| e^{j\phi} = 0. \tag{8}$$

Which means that

$$|r_1| = |r_2| \Rightarrow \tanh(\kappa_1 L_1) = \tanh(\kappa_2 L_2) \Rightarrow \kappa_1 L_1 = \kappa_2 L_2$$
$$\phi = \pi + 2k\pi \tag{9}$$

So the generalized conditions for a PS-FBG functioning as a first-order OD are $\kappa_1 L_1 = \kappa_2 L_2$ and $\phi = \pi + 2k\pi$ .

Then the field reflectivity $r$ in a limited bandwidth around the resonance notch can be rewritten as:

$$r = jA_0\sigma = jA_1(\omega - \omega_0) \tag{10}$$

Where $A_0$ and $A_1$ are both constants.

From Eq. (7), in terms of the field transmittance $t$, it can also be inferred that in order to approach the spectral response that is required for first-order OI, the two following specifications are necessary:

(i) $1 + |r_1||r_2| e^{j\phi} = 0$, which means that $|r_1| \approx |r_2| \approx 1$ and $\phi = \pi + 2k\pi$ .

(ii) $|r_1||r_2|\sigma << \kappa_1 |r_1| + \kappa_2 |r_2|$ , which can be easily meet when the coupling coefficient $\kappa_1, \kappa_2$ is large enough. Then the second-order term can be neglected as compared with the first-order term.

So the generalized conditions for a PS-FBG functioning as a first-order OI are $|r_1| \approx |r_2| \approx 1$ , $\phi = \pi + 2k\pi$ and $\sigma << \kappa_1, \kappa_2$ , which is equivalent to the conditions proposed in Ref. [12].

Then the field transmittance $t$ in a limited bandwidth around the resonance notch can be rewritten as:

$$t = \frac{A_3}{j\sigma} = \frac{A_4}{j(\omega - \omega_0)} \tag{11}$$

Where $A_3$ and $A_4$ are both constants.

From the above analysis, we can know that a PS-FBG can perform as a first-order OD and first-order OI simultaneously when it meets that $|r_1| = |r_2| \approx 1$ , $\phi = \pi + 2k\pi$ and $\sigma << \kappa_1, \kappa_2$ .

## 3. Numerical results

In order to verify the above conclusions, to begin with, we numerically prove that for functioning as an ideal first-order OD the specification imposed in Ref. [7] (the two uniform FBGs in the structure must be identical ( $L_1 = L_2 = L$ and $\kappa_1 = \kappa_2 = \kappa$ ), $\phi = \pi$ )is not strictly necessary and the generalized conditions for this operation are $\kappa_1 L_1 = \kappa_2 L_2$ and $\phi = \pi + 2k\pi$ .

So we simulate the reflective spectral response of a PS-FBG1 when the coupling coefficient of each section is $\kappa_1 = 1400m^{-1}$ and $\kappa_2 = 2800m^{-1}$ while the length of each section is $L_1 = 2mm$ and $L_2 = 1mm$ . The Bragg wavelength is $\lambda_B = 1550nm$ , and the effective refractive index is $n_{eff} = 1.46$ , and with an exact π phase shift between the two grating sections. In this case, the coupling coefficient and the length of each section are not the same, but the product of them are the same. Using transfer matrix method, we can get the reflective spectral response of the PS-FBG, which is shown in Fig. 2. Fig. 2 illustrates that the amplitude response of this PS-FBG is linear dependence on the angular baseband frequency in a limited bandwidth around the central wavelength and the phase response has a pi shift in the central wavelength, which is in good agreement with the conditions for performing as an ideal OD in a limited bandwidth.

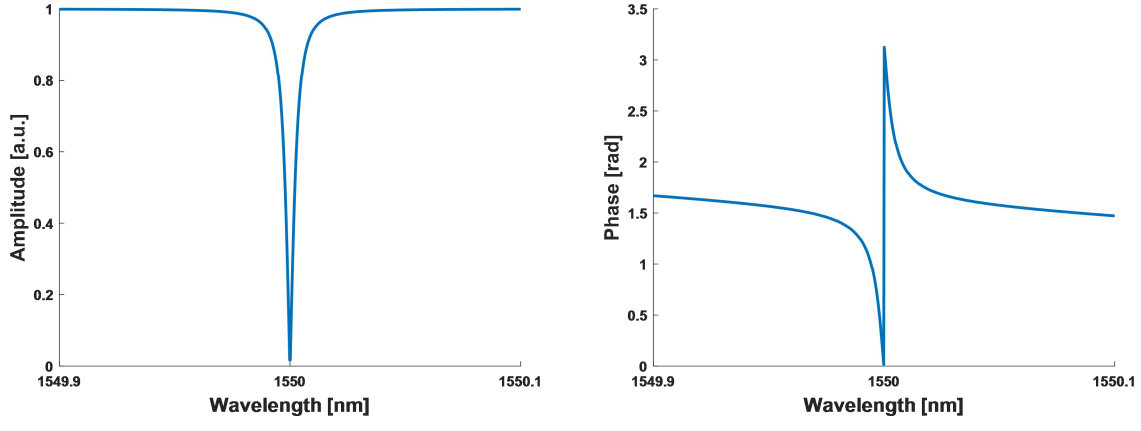


Fig. 2. Numerically simulated (a) amplitude and (b) phase responses of PS-FBG1.

Fig. 3 shows the differentiation results when a 5 ns FWHM Gaussian pulse launched to the above designed PS-FBG1. We can clearly see that the obtained output results are in very good agreement with the ideal output results, which confirms the

This article has been accepted for publication in a future issue of this journal, but has not been fully edited. Content may change prior to final publication. Citation information: DOI 10.1109/JPHOT.2018.2824661, IEEE Photonics Journal

generalized conditions ( $\kappa_1 L_1 = \kappa_2 L_2$ and $\phi = \pi + 2k\pi$ ) for differentiation.

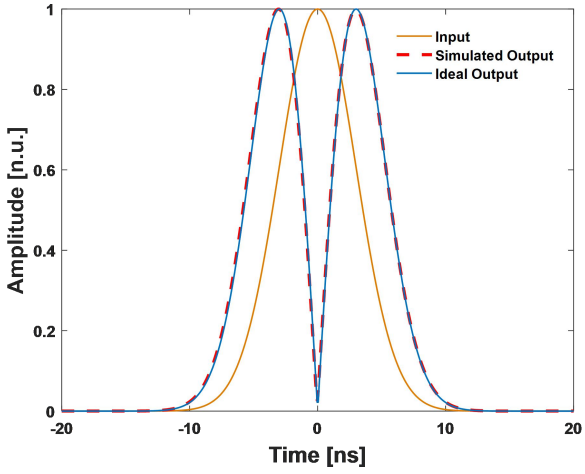


Fig. 3. Temporal response of the PS-FBG1 in Fig. 2: Gaussian 5 ns-FWHM input pulse (yellow solid line), simulated output pulse (red dotted line) and ideal expected output (blue solid line).

Then we numerically prove that a PS-FBG can perform as a first-order OD and first-order OI simultaneously when it meets the condition: $|r_1| = |r_2| \approx 1$ , $\phi = \pi + 2k\pi$ and $\sigma << \kappa_1, \kappa_2$ .

For PS-FBG2, the coupling coefficient of each section ( $\kappa_1 = \kappa_2$ ) is selected as 1500 $m^{-1}$, 2500$m^{-1}$ and 3500$m^{-1}$, respectively, while the length of each section is $L_1 = L_2 = 1mm$ . The other parameters remain the same as PS-FBG1. Fig. 4 shows the numerically simulated amplitude $|r|$ and phase $r_\theta$ responses of the field reflectivity. Fig. 5 shows the numerically simulated amplitude $|t|$ and phase $t_\theta$ responses of the field transmittance. Fig. 4 illustrates that the differentiation bandwidth of the amplitude response of field reflectivity decreases while the phase always has a pi shift in the center wavelength when the coupling coefficient increases from 1500 $m^{-1}$ to 2500$m^{-1}$ to 3500$m^{-1}$. However, Fig. 5 shows that the amplitude response and the phase response of the field transmittance both approach more to the ideal OI's amplitude and phase responses when the coupling coefficient increases from 1500 $m^{-1}$ to 2500$m^{-1}$ to 3500$m^{-1}$. Those mean that when the coupling coefficient of each section is 3500$m^{-1}$ (at this coupling coefficient, the reflectivity $|r_1| = |r_2| \approx 1$ ), the designed PS-FBG can function as the OD and OI at the same time.

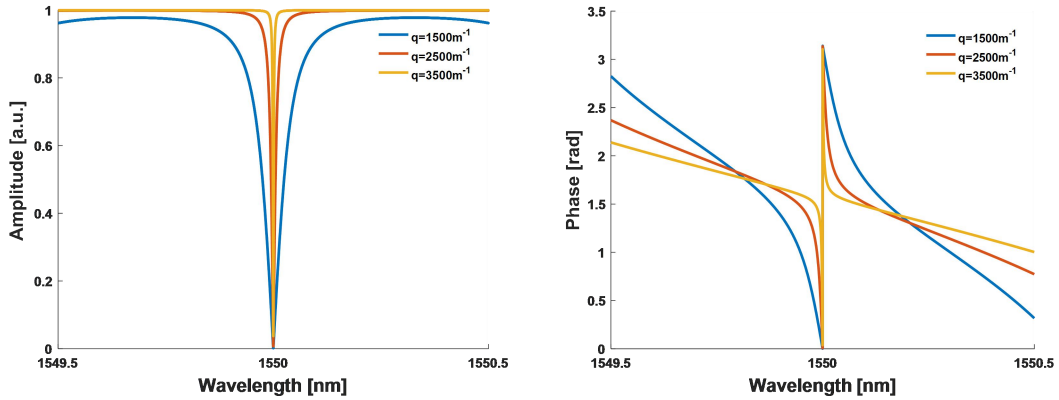


Fig. 4. Numerically simulated (a) amplitude and (b) phase responses of the field reflectivity of PS-FBG2.

This article has been accepted for publication in a future issue of this journal, but has not been fully edited. Content may change prior to final publication. Citation information: DOI 10.1109/JPHOT.2018.2824661, IEEE Photonics Journal

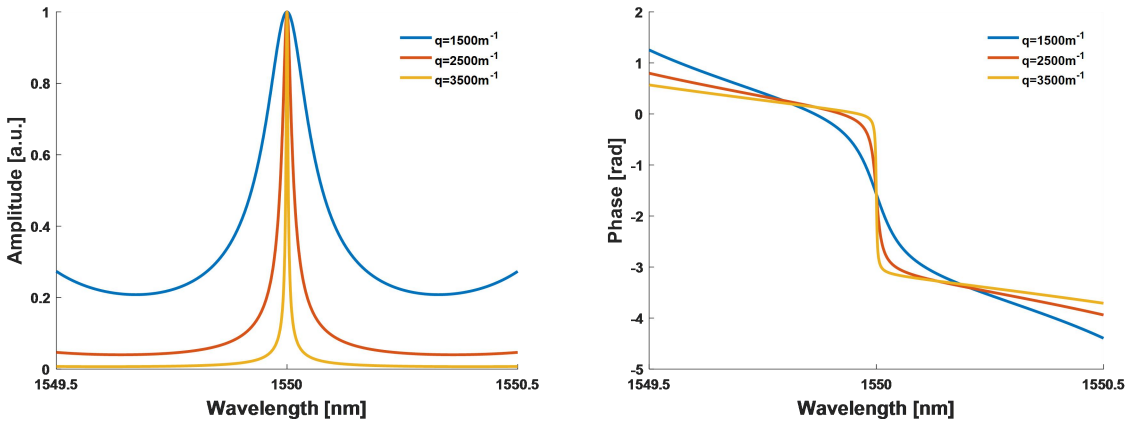


Fig. 5. Numerically simulated (a) amplitude and (b) phase responses of the field transmittance of PS-FBG2.

Therefore, we set the coupling coefficient $\kappa_1 = \kappa_2 = 3500m^{-1}$ and numerically demonstrate the functionality of the PS-FBG3. The obtained results are shown in Fig. 6. Fig. 6(a) shows the temporal differentiation results when a 10 ns FWHM Gaussian pulse launched to the designed PS-FBG3, while Fig. 6(b) shows the integration results when a 10 ps FWHM Gaussian pulse launched to the designed PS-FBG3. Fig. 6 clearly illustrates that the output results of the designed differentiator and integrator are both in very good agreement with the ideal output results, which further confirms that the PS-FBG3 can function as the OD and OI simultaneously in a high accuracy.

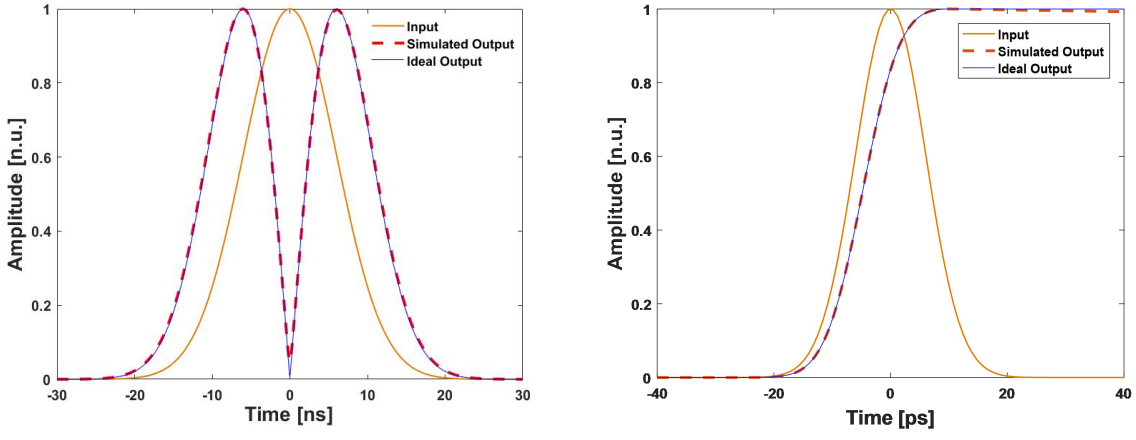


Fig. 6. Temporal responses of the PS-FBG3 (a) for differentiation, Gaussian 10 ns-FWHM input pulse (yellow solid line), simulated output pulse (red dotted line) and ideal expected output (blue solid line); (b) for differentiation, Gaussian 10 ps-FWHM input pulse (yellow solid line), simulated output pulse (red dotted line) and ideal expected output (blue solid line).

## 4. Conclusions

In conclusion, analytically and numerically, we have demonstrated a practically realizable phase-shift fiber Bragg grating can function as a first-order optical differentiator and a first-order optical integrator at the same time. The required conditions for the phase-shifted fiber Bragg grating are $|r_1| = |r_2| \approx 1$ , $\phi = \pi + 2k\pi$ and $\sigma << \kappa_1, \kappa_2$ . The PS-FBG working in reflection implements the optical differentiation while the PS-FBG working in transmission implements the optical integration. The processing speed of the PS-FBG for differentiation is a few gigahertz and for integration is hundreds of gigahertzes. The accuracy of the device for differentiation and integration are both very high and it may have some potential applications in the future all-optical signal processing. We also provide the generalized conditions for a PS-FBG functioning as a first-order optical differentiator are ( $\kappa_1 L_1 = \kappa_2 L_2$ and $\phi = \pi + 2k\pi$ ) and functioning as a first-order optical are ( $|r_1| \approx |r_2| \approx 1$ , $\phi = \pi + 2k\pi$ and $\sigma << \kappa_1, \kappa_2$ ), respectively. In addition, we can use the concatenation of such PS-FBG to implement the high-order differentiators and integrators simultaneously.

## Acknowledgements

This work is supported by National Natural Science Foundation of China (NSFC) (61775074), Natural Science Foundation of Guangdong Province, China (2015A030313633), Key Project of Department of Education of Guangdong Province (2014KTSCX153) and Fundamental Research Funds of Foshan University (2014042).

## References

[1] J. Azaña, “Ultrafast analog all-optical signal processors based on fiber-grating devices,” IEEE Photon. J. 2, 359–386 (2010).
[2] N. Q. Ngo, S. F. Yu, S. C. Tjin, and C. H. Kam, “A new theoretical basis of higher-derivative optical differentiators,” Opt. Commun. 230, 115–129 (2004).
[3] N. Q. Ngo, "Optical integrator for optical dark-soliton detection and pulse shaping," Applied optics 45, 6785-6791 (2006).
[4] Y. Park, J. Azaña, and R. Slavík, “Ultrafast all-optical first- and higher-order differentiators based on interferometers,” Opt. Lett. 32, 710–712 (2007).
[5] M. Kulishov and J. Azana, "Long-period fiber gratings as ultrafast optical differentiators," Optics Letters 30, 2700-2702 (2005).
[6] R. Slavík, Y. Park, M. Kulishov, R. Morandotti, and J. Azaña, “Ultrafast all-optical differentiators,” Opt. Express 14, 10699–10707 (2006).
[7] N. K. Berger, B. Levit, B. Fischer, M. Kulishov, D. V. Plant, and J. Azaña, "Temporal differentiation of optical signals using a phase-shifted fiber Bragg grating," Optics Express 15, 371-381 (2007).
[8] L. M. Rivas, K. Singh, A. Carballar, and J. Azana, "Arbitrary-Order Ultrabroadband All-Optical Differentiators Based on Fiber Bragg Gratings," IEEE Photonics Technology Letters 19, 1209-1211 (2007).
[9] Mykola Kulishov and José Azaña, "Design of high-order all-optical temporal differentiators based on multiple-phase-shifted fiber Bragg gratings," Opt. Express15, 6152-6166 (2007)
[10] N. Q. Ngo, "Design of an optical temporal integrator based on a phase-shifted fiber Bragg grating in transmission," Optics letters 32, 3020-3022 (2007).
[11] M. H. Asghari and J. Azaña, "Proposal for arbitrary-order temporal integration of ultrafast optical signals using a single uniform-period fiber Bragg grating," Optics letters 33, 1548-1550 (2008).
[12] M. H. Asghari and J. Azaña, "Design of all-optical high-order temporal integrators based on multiple-phase-shifted Bragg gratings," Optics express 16, 11459-11469 (2008).
[13] J. Azaña, "Proposal of a uniform fiber Bragg grating as an ultrafast all-optical integrator," Optics letters 33, 4-6 (2008).
[14] F. Liu, T. Wang, L. Qiang, T. Ye, Z. Zhang, M. Qiu, and Y. Su, “Compact optical temporal differentiator based on silicon microring resonator,” Opt. Express 16, 15880–15886 (2008).
[15] J. Dong, A. Zheng, D. Gao, S. Liao, L. Lei, D. Huang, and X. Zhang, "High-order photonic differentiator employing on-chip cascaded microring resonators," Opt Lett 38, 628-630 (2013).
[16] A. Zheng, J. Dong, L. Zhou, X. Xiao, Q. Yang, X. Zhang, and J. Chen, "Fractional-order photonic differentiator using an on-chip microring resonator," Optics Letters 39, 6355 (2014).
[17] M. Ferrera, Y. Park, L. Razzari, B. E. Little, S. T. Chu, R. Morandotti, D. J. Moss, and J. Azana, "On-chip CMOS-compatible all-optical integrator," Nat Commun 1, 29 (2010).
[18] W. Liu, M. Li, R. S. Guzzon, E. J. Norberg, J. S. Parker, M. Lu, L. A. Coldren, and J. Yao, "A fully reconfigurable photonic integrated signal processor," Nature Photonics 10, 190 (2016).
[19] A. Papoulis, The Fourier Integral and Its Applications. New York, NY, USA: McGraw-Hill, 1960.
[20] T. Erdogan, "Fiber grating spectra," Journal of Lightwave Technology 15, 1277-1294 (1997).